Graphene Bilayer Structures with Superfluid Magnetoexcitons

A. A. Pikalov · D. V. Fil

Abstract We study superfluid behavior of a gas of spatially indirect magnetoexcitons with reference to a system of two graphene layers embedded in a multilayer dielectric structure. The system is considered as an alternative of a double quantum well in a GaAs heterostructure. We determine a range of parameters (interlayer distance, dielectric constant, magnetic field and gate voltage) where magnetoexciton superfluidity can be achieved. Temperature of superfluid transition is computed. A reduction of critical parameters caused by impurities is evaluated and critical impurity concentration is determined.

1 Introduction

Recent progress in creation of heterostuctures with two graphene layers separated by a thin dielectrics [1] opens possibilities to use graphene for creation of multiple quantum well structures with separately accessed conducting layers. In [1] SiO_2 substrate and Al_2O_3 internal dielectric layer were used. Another promising dielectric is hexagonal BN [2]. It has a number of advantages, such as an atomically smooth surface that is free of dangling bonds and charge traps, a lattice constant similar to that of graphite, and a large electronic bandgap.

The attention to graphene heterostructures is caused, in some part, by the idea to use them for a realization of superfluidity of spatially indirect excitons [3,4,5, 6,7,8,9]. Bound electron-hole pairs cannot carry electrical charge, but in bilayers they can provide a flow of oppositely directed electrical currents. Therefore, exciton superfluidity in bilayers should manifest itself as a special kind of superconductivity - the counterflow one, that means infinite conductance under a flow of equal in modulus and oppositely directed currents in the layers.

A. A. Pikalov · D. V. Fil
Institute for Single Crystals, National Academy of Sciences of Ukraine, Lenin ave. 60 Kharkov 61001, Ukraine
Tel.: +38-057-3410492
E-mail: fil@isc.kharkov.ua

The idea on counterflow superconductivity with reference to electron-hole bilayers was put forward in [10,11]. The attempts to observe counterflow conductivity directly were done [12,13,14] for bilayer quantum Hall systems realized in GaAs heterostructures. In the latter systems superconducting behavior might be accounted for magnetoexcitons [15,16]. The effect is expected for the filling factors of Landau levels $\nu_i = 2\pi\ell^2 n_i$ ($\ell = \sqrt{\hbar c/eB}$ is magnetic length, n_i is the electron density in the i-th layer) satisfying the condition $\nu_1 + \nu_2 = 1$. The role of holes is played by empty states in zero Landau level. In experiments [12,13,14] an exponential increase of the counterflow conductivity under lowering of temperature was observed, but zero-resistance state was not achieved. The latter can be explained by the presence of unbound vortices [17,18,19]. Such vortices may appear due to spatial variation of the electron density caused by disorder.

To demonstrate counterflow superconductivity quantum Hall bilayers should have the parameters that satisfy two additional conditions: $d \lesssim \ell$ and $\ell \lesssim a_B^*$, where d is the interlayer distance, and $a_B^* = \varepsilon\hbar^2/e^2 m^*$ is the effective Bohr radius (ε is the dielectric constant of the matrix, and m^* is the effective electron mass). The first inequality comes from the dynamical stability condition. For balanced bilayers ($\nu_1 = \nu_2$) the mean-fields theory yields $d < 1.175\ell$. The second inequality is the condition for the Coulomb energy $e^2/\varepsilon\ell$ be smaller than the energy distance between Landau levels. In GaAs $a_B^* \approx 10$ nm and the condition $\ell \lesssim a_B^*$ is fulfilled at rather strong magnetic fields $B \gtrsim 6$ T (actually, the experiments [12,13,14] were done at smaller fields). At $d \lesssim 10$ nm the interlayer tunneling is not negligible small and may result in a locking of the bilayer for the counterflow transport at small input current [20,21]. At larger input current the system unlocks, but the state becomes nonstationary one [22,23,24] that is accompanied by a dissipation (the power of losses is proportional to the square of the amplitude of the interlayer tunneling [22,24]).

The idea to use graphene for the realization of electron-hole superfluidity in quantum Hall bilayers [6,7,8,9] looks very attractive. The distance between Landau Levels in monolayer graphene is proportional to the inverse magnetic length, magnetic field does not enter into the condition of smallness of the Coulomb energy, and small magnetic fields can be used. Smaller magnetic fields correspond to smaller critical temperature, but, at the same time, they correspond to larger critical d. Use of large d allows to suppress completely negative effects caused by interlayer tunneling.

In this paper we concentrated on three questions. First, we determine, in what range of internal parameters and external fields magnetoexciton superfluidity can be realized. Second, we evaluate critical temperature for pure system. Third, we consider its reduction caused by electron-impurity interaction. Our study extends the results of [8], where a system of two graphene layers embedded into a bulk dielectric matrix was considered. Here we investigate structures with one and two graphene layers situated at the surface.

2 Conditions for the electron-hole pairing in zero Landau level

Quantum Hall effect in graphene is characterized by unusual systematics of Landau levels and the additional four-fold degeneracy connected with two valleys and two spin projections [25]. The energies of Landau levels in graphene are $E_{\pm N} =$

$\frac{\hbar v_F}{\ell}\sqrt{2|N|}$, where $N = 0, 1, 2, \ldots$, and $v_F \approx 10^6$ m/s is the Fermi velocity. In a free standing graphene the $N = 0$ Landau level is half-filled. A state with only completely filled Landau levels corresponds to a plateau at the Hall conductivity plot (dependence of σ_{xy} on electron density). A free standing graphene is just between two plateaus [26]. A given quantum states in zero Landau is characterized by the guiding center index X and the combination of the spin and valley indexes. Below we call four possible combinations, the components, and numerate them by the index $\beta = 1, 2, 3, 4$.

We describe electron-hole pairing in zero Landau level in graphene by the wave function that is a generalization of the wave function [15] to the multicomponent case

$$|\Psi\rangle = \prod_\beta \prod_X (u_\beta c_{1\beta X}^+ + v_\beta c_{2\beta X}^+)|0\rangle. \tag{1}$$

Here $c_{i\beta X}^+$ is the electron creation operator (the operator that fills a given state in $N = 0$ Landau Level), $|0\rangle$ is the state with empty zero level, i is the layer index. The $u - v$ coefficients satisfy the condition $|u_\beta|^2 + |v_\beta|^2 = 0$. The function (1) can be rewritten in the form

$$|\Psi\rangle = \prod_\beta \prod_X (u_\beta + v_\beta c_{2\beta X}^+ h_{1\beta X}^+)|vac1\rangle, \tag{2}$$

where $h_{1\beta X}^+ = c_{1\beta X}$ is the hole creation operator, and the vacuum state is defined as $|vac1\rangle = \prod_\beta \prod_X c_{1\beta X}^+|0\rangle$. One can see that the function (2) is an analog of the BCS function in the Bardin-Cooper-Schrieffer theory of superconductivity.

The quantity $\tilde{\nu}_\beta = |u_\beta|^2 - |v_\beta|^2$ gives the filling factor imbalance for the component β. The order parameter of the electron-hole pairing reads as $\Delta_\beta = u_\beta^* v_\beta = \sqrt{1 - \tilde{\nu}_\beta^2}e^{i\varphi}/2$. If a given component is maximally imbalanced ($\tilde{\nu}_\beta = \pm 1$) the order parameter Δ_β is equal to zero.

If a one component bilayer system is balanced, the order parameter for the electron-hole pairing is maximum. But if the number of components is even, the balance $\sum_\beta \tilde{\nu}_\beta = 0$ can be reached at $\tilde{\nu}_\beta = 1$ for half of the components and $\tilde{\nu}_\beta = -1$ for the other half. In the latter case all $\Delta_\beta = 0$. As is shown below, just such a state corresponds to the energy minimum. In other words, in balanced graphene bilayers electron-hole pairing does not occur.

At nonzero imbalance $\sum_\beta \tilde{\nu}_\beta \neq 0, \pm 2, \pm 4$ at least for one component $\tilde{\nu}_\beta \neq \pm 1$, and electron-hole pairing may occur. Nonzero imbalance can be provided by electrical field directed perpendicular to the layers. Such a field can be created by a voltage difference applied between top and bottom gates (see fig. 1).

We consider the general structure "dielectric 1 - graphene 1 - dielectric 2 - graphene 2 - dielectric 3" with three different dielectric constants ε_1, ε_2 and ε_3. Dielectrics 1 and 3 are assumed to be thick (much thicker than the distance between graphene layers d). Solving the standard electrostatic problem we obtain the Fourier components of the Coulomb interaction $V_{ii'}$ for the electrons located in i and i' graphene layers

$$V_{11}(\mathbf{q}) = \frac{4\pi e^2}{q} \frac{\varepsilon_2 + \varepsilon_3 + (\varepsilon_2 - \varepsilon_3)e^{-2qd}}{(\varepsilon_2 + \varepsilon_3)(\varepsilon_2 + \varepsilon_1) - (\varepsilon_2 - \varepsilon_3)(\varepsilon_2 - \varepsilon_1)e^{-2qd}}, \tag{3}$$
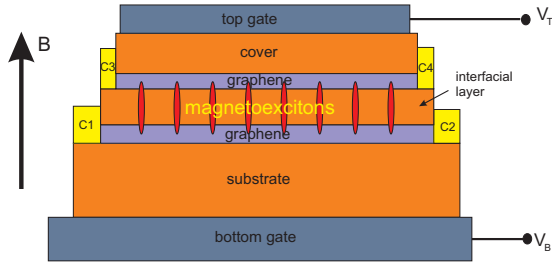
Fig. 1 Schematic view of the system under study. C1 - C4 are the contacts.

$$V_{22}(\mathbf{q}) = \frac{4\pi e^2}{q} \frac{\varepsilon_2 + \varepsilon_1 + (\varepsilon_2 - \varepsilon_1)e^{-2qd}}{(\varepsilon_2 + \varepsilon_3)(\varepsilon_2 + \varepsilon_1) - (\varepsilon_2 - \varepsilon_3)(\varepsilon_2 - \varepsilon_1)e^{-2qd}}, \tag{4}$$

$$V_{12}(\mathbf{q}) = \frac{8\pi e^2}{q} \frac{\varepsilon_2 e^{-qd}}{(\varepsilon_2 + \varepsilon_3)(\varepsilon_2 + \varepsilon_1) - (\varepsilon_2 - \varepsilon_3)(\varepsilon_2 - \varepsilon_1)e^{-2qd}}. \tag{5}$$

For electrons in $N = 0$ Landau level in graphene the Hamiltonian of Coulomb interaction has the form

$$H_C = \frac{1}{2S} \sum_{i,i'} \sum_{X,X'} \sum_{\beta,\beta'} \sum_{\mathbf{q}} V_{ii'}(\mathbf{q}) e^{-\frac{q^2\ell^2}{2} + iq_x(X'-X)}$$
$$c^+_{i\beta X + q_y\ell^2/2} c^+_{i'\beta' X' - q_y\ell^2/2} c_{i'\beta' X' + q_y\ell^2/2} c_{i\beta X - q_y\ell^2/2}, \tag{6}$$

where S is the area of the system. The interaction with the gate field is described by the Hamiltonian

$$H_G = -\frac{eV_g}{2} \sum_{X\beta} \left(c^+_{1\beta X} c_{1\beta X} - c^+_{2\beta X} c_{2\beta X} \right), \tag{7}$$

where V_g is the interlayer voltage created by the external gate (bare voltage).

Rewriting the wave function (1) in the form

$$|\Psi\rangle = \prod_X \prod_\beta \left(\cos\frac{\theta_\beta}{2} c^+_{1\beta X} + e^{i\varphi_\beta} \sin\frac{\theta_\beta}{2} c^+_{2\beta X} \right) |0\rangle, \tag{8}$$

and computing the energy in the state (8) we obtain

$$E_{mf} = \frac{S}{8\pi\ell^2} \left(W \sum_{\beta\beta'} \cos\theta_\beta \cos\theta_{\beta'} - J_0 \sum_\beta \cos^2\theta_\beta - (2eV_g + J_z) \sum_\beta \cos\theta_\beta \right), \tag{9}$$

where $W = e^2 d/\varepsilon_2\ell^2$ is the energy of direct Coulomb interaction. The exchange interaction energies

$$J_{ik} = \frac{1}{2\pi} \int_0^\infty q V_{ik}(q) e^{-\frac{q^2\ell^2}{2}} dq$$

determine the parameters $J_0 = (J_{11} + J_{22})/2 - J_{12}$ and $J_z = J_{11} - J_{22}$. The relation between θ_β and $\tilde{\nu}_\beta$ is given by equation $\tilde{\nu}_\beta = \cos\theta_\beta$.

Taking into account the inequalities $W > J_0$, and $J_{11}, J_{22} > J_{12}$ (that can be checked directly) we find that at $V_g = 0$ the minimum of (9) is reached at

$\tilde{\nu}_1 = \tilde{\nu}_2 = 1$, $\tilde{\nu}_3 = \tilde{\nu}_4 = -1$. It indicates the absence of electron-hole pairing in balanced systems.

If $V_g \neq 0$ and belongs to one of the intervals

$$nW + J_{22} - J_{12} < eV_g < (n+2)W - J_{11} + J_{12}, \tag{10}$$

where $n = -4, -2, 0, 2$, the energy minimum is reached at $\tilde{\nu}_{\beta_a} \neq \pm 1$ for one of the components. We will call such a component the active one.

Let us, for instance, consider the interval (10) with $n = 0$. Then the energy minimum is reached at

$$\tilde{\nu}_{\beta_a} = \frac{eV_g + J_z/2 - W}{W - J_0}.$$

The case $\tilde{\nu}_{\beta_a} = 0$ (with maximum order parameter) corresponds to the voltage

$$eV_g = -\frac{J_z}{2} + W. \tag{11}$$

Eq. (11) determines the relation between magnetic field and the gate voltage V_g. To keep $\tilde{\nu}_{\beta_a} = 0$ the gate voltage should be varied synchronically with B. In particular, at $J_z = 0$ ($\varepsilon_1 = \varepsilon_3$) the quantities V_g and B are linearly related:

$$V_g = \frac{\alpha d B c}{\varepsilon_2}, \tag{12}$$

where $\alpha \approx 1/137$ is the fine structure constant (the relation (12) is given in SI units).

If only the gate voltage or magnetic field is varied, the order parameter (and the critical temperature) changes nonmonotonically reaching the maximum at the point determined by (11).

3 Collective mode spectrum and phase diagram

The components that belong completely to one layer do not take part in the pairing. In what follows we consider the dynamics of only the active component.

We describe the active component by the wave function

$$|\Psi\rangle = \prod_X \left(\cos\frac{\theta_X}{2} c^+_{1, X+Q_y\ell^2/2} + e^{i(Q_x X + \tilde{\varphi}_X)} \sin\frac{\theta_X}{2} c^+_{2, X-Q_y\ell^2/2} \right) |0\rangle \tag{13}$$

(here and below we omit the component index). Eq. (13) describes the state with nonzero counterflow currents. To illustrate this statement we neglect for a moment the order parameter fluctuations ($\tilde{\varphi}_X = 0$, $\theta_X = \theta_a$).

The order parameter is determined by the equation

$$\Delta(\mathbf{r}) = \sum_{X, X'} \psi_X^*(\mathbf{r}) \psi_{X'}(\mathbf{r}) \langle \Psi | c^+_{1,X} c_{2,X'} | \Psi \rangle. \tag{14}$$

where

$$\psi_X(\mathbf{r}) = \frac{1}{\pi^{1/4}\sqrt{\ell L_y}} e^{-i\frac{Xy}{\ell^2}} e^{-\frac{(x-X)^2}{2\ell^2}}$$

is the single-particle wave function in the coordinate representation, L_y is the width of the system. Substitution (13) into (14) yields

$$\Delta(\mathbf{r}) = \frac{\sin\theta_a}{2} e^{-\frac{Q^2\ell^2}{2}} e^{i\mathbf{Q}\cdot\mathbf{r}}. \tag{15}$$

One can see from Eq. (15) that $\mathbf{Q} = (Q_x, Q_y)$ is the gradient of the phase of the order parameter.

Computing the energy in the state (13) and neglecting the fluctuations we obtain

$$E_0 = \frac{S}{8\pi\ell^2}\left([W - F_S(0)]\cos^2\theta_a - F_D(Q)\sin^2\theta_a\right), \tag{16}$$

where

$$F_S(q) = \frac{1}{4\pi}\int_0^\infty p J_0(pq\ell^2)[V_{11}(p) + V_{22}(p)]e^{-\frac{p^2\ell^2}{2}}dp, \tag{17}$$

and

$$F_D(q) = \frac{1}{2\pi}\int_0^\infty p J_0(pq\ell^2)V_{12}(p)e^{-\frac{p^2\ell^2}{2}}dp. \tag{18}$$

Electrical currents can be found from a variation of the energy caused by a variation of the vector-potential

$$\delta E = -\frac{1}{c}\int d^2r \sum_i \mathbf{j}_i\delta\mathbf{A}_i. \tag{19}$$

Here $\mathbf{A}_i$ is the in-plane component of the vector-potential in the layer i. To obtain the explicit expression for the variation (19) we replace the phase gradient in (16) with the gauge-invariant expression $\mathbf{Q} - \frac{e}{\hbar c}(\mathbf{A}_{pl,1} - \mathbf{A}_{pl,2})$, where $\mathbf{A}_{pl,i}$ is the parallel to the graphene layers component of the vector potential in the layer i. Then, using (19) one finds the currents

$$\mathbf{j}_1 = -\mathbf{j}_2 = -\frac{e}{\hbar}\frac{\sin^2\theta_a}{8\pi\ell^2}\frac{dF_D(Q)}{d\mathbf{Q}}. \tag{20}$$

At small gradients $Q\ell \ll 1$ Eq. (20) is reduced to

$$j_1 = \frac{e}{\hbar}\rho_{s0}Q, \tag{21}$$

where coefficient of proportionality between the current and the phase gradient

$$\rho_{s0} = \frac{\ell^2}{32\pi^2}\sin^2\theta_a\int_0^\infty p^3 V_{12}(p)e^{-\frac{p^2\ell^2}{2}}dp \tag{22}$$

is called the zero temperature superfluid stiffness (the definition is given in the next section). Since we neglect fluctuations, the expression (20) yields the current at $T = 0$.

Implying the fluctuations of the amplitude and the phase of the order parameter are small one can present the energy as

$$E = E_0 + E_2 + \dots \tag{23}$$

The quadratic in fluctuations term can be diagonalized:

$$E_2 = \sum_q [m_z(-q)K_{zz}(q)m_z(q) + \frac{1}{4}\varphi(-q)K_{\varphi\varphi}(q)\varphi(q)$$

$$-\frac{1}{2}(im_z(-q)K_{z\varphi}(q)\varphi(q) + c.c.)], \tag{24}$$

where

$$m_z(q) = \frac{1}{2}\sqrt{\frac{2\pi l^2}{S}}\sum_X (\cos\theta_X - \cos\theta_a)\, e^{-iqX},$$

$$\varphi(q) = \sqrt{\frac{2\pi l^2}{S}}\sum_X \tilde{\varphi}(X)e^{-iqX} \tag{25}$$

are the Fourier components of the fluctuations.

Eqs. (24) yields the energy of fluctuations with the wave vector directed along the x axis. The component of the matrix K can be presented in form independent of the choice of the direction of the coordinate axes

$$K_{zz}(\mathbf{q}, \mathbf{Q}) = H(\mathbf{q}, \mathbf{Q}) - F_S(|\mathbf{q}|) + F_D(|\mathbf{Q}|) + \Xi(\mathbf{q}, \mathbf{Q})\cot^2\theta_a,$$

$$K_{\varphi\varphi}(\mathbf{q}, \mathbf{Q}) = \sin^2\theta_a \Xi(\mathbf{q}, \mathbf{Q}),$$

$$K_{z\varphi}(\mathbf{q}, \mathbf{Q}) = -\cos\theta_a[F_D(|\mathbf{q} + \mathbf{Q}|) - F_D(|\mathbf{q} - \mathbf{Q}|)]/2, \tag{26}$$

where

$$H(\mathbf{q}, \mathbf{Q}) = \frac{1}{2\pi\ell^2}\left[\frac{V_{11}(\mathbf{q}) + V_{22}(\mathbf{q})}{2} - V_{12}(\mathbf{q})\cos\left(|\mathbf{q}\times\mathbf{Q}|\ell^2\right)\right]e^{-\frac{q^2\ell^2}{2}}$$

$$\Xi(\mathbf{q}, \mathbf{Q}) = \left[F_D(|\mathbf{Q}|) - \frac{F_D(|\mathbf{q} + \mathbf{Q}|) + F_D(|\mathbf{q} - \mathbf{Q}|)}{2}\right]. \tag{27}$$

The quantities $K_{\alpha\beta}(q)$ in (24) are expressed in terms of (26) as $K_{\alpha\beta}(q) = K_{\alpha\beta}(\mathbf{q}, \mathbf{Q})\big|_{\mathbf{q}=q\mathbf{i}_x}$.

The quantity $\hbar\cos\theta_X/2$ can be treated as a z-component of the pseudospin and it is canonically conjugated with the phase φ_X. The Fourier transformed quantities (25) are defined as canonical variables as well. The equations of motion for the quantities $m_z(q)$ and $\varphi(q)$ read as

$$\hbar\frac{d\varphi(q)}{dt} = 2K_{zz}(q)m_z(q) - iK_{z\varphi}(q)\varphi(q),$$

$$\hbar\frac{dm_z(q)}{dt} = -\frac{1}{2}K_{\varphi\varphi}(q)\varphi(q) - iK_{z\varphi}(q)m_z(q). \tag{28}$$

Eqs. (28) yield the collective mode spectrum $\Omega(q, \mathbf{Q}) = \sqrt{K_{\varphi\varphi}(q)K_{zz}(q)} + K_{z\varphi}(q)$. Rotating the axes one obtains the excitation spectrum at general $\mathbf{q}$

$$\Omega(\mathbf{q}, \mathbf{Q}) = \sqrt{K_{\varphi\varphi}(\mathbf{q}, \mathbf{Q})K_{zz}(\mathbf{q}, \mathbf{Q})} + K_{z\varphi}(\mathbf{q}, \mathbf{Q}). \tag{29}$$

At $\mathbf{Q} = 0$ the spectrum (29) is isotropic. It can be presented in the Bogolyubov form

$$\Omega_0(q) = \sqrt{\varepsilon_q(\varepsilon_q + \gamma_q)}. \tag{30}$$

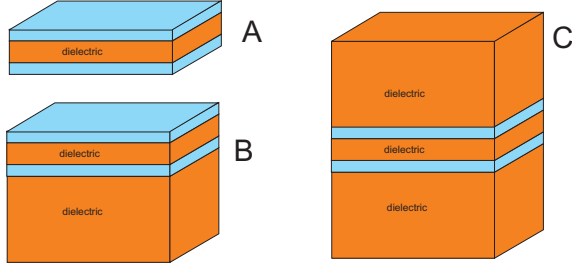In Eq. (30)

$$\varepsilon_q = F_D(0) - F_D(q) \tag{31}$$

Fig. 2 Graphene hererostructures under study.

is the kinetic energy ($\varepsilon_q \approx \hbar^2 q^2 / 2M$ at $q\ell \ll 1$, where M is the magnetoexciton mass, see, for instance [27]), and

$$\gamma_q = [H(\mathbf{q}, 0) - F_S(q) + F_D(q)] \sin^2 \theta_0 \tag{32}$$

has the sense of the exciton-exciton interaction energy (that includes the direct and exchange parts).

The condition for the dynamical stability of the state (13) is the real valueness of the excitation spectrum (30). This condition determines the diapason of d/ℓ and ε_i where superfluid magnetoexciton state can be realized. To be more concrete we consider three types of heterostructures. Type A is a graphene-dielectric-graphene sandwich with two graphene layers at the surface, type B is a graphene-dielectric-graphene-dielectric structure with one such a layer, and type C is a system of two graphene layers embedded in a dielectric matrix (Fig. 2). For simplicity, we imply the same dielectric constants ε for the interfacial layer and the substrate.

The dynamical stability condition is fulfilled at $0 < d/\ell < \tilde{d}_c(\varepsilon)$, where $\tilde{d}_c(\varepsilon)$ depends on the imbalance parameter $\tilde{\nu}_{\beta_a} \equiv \tilde{\nu}_a$. The dependence $\tilde{d}_c(\varepsilon)$ at $\tilde{\nu}_a = 0$ is shown in Fig. 3.

The requirement for the Coulomb energy be smaller than the distance between Landau levels yields the restriction on ε. Since we study the pairing in $N = 0$ Landau level we compare the Coulomb energy with the energy distance between $N = 0$ and $N = 1$ levels $\omega_c = \sqrt{2}\hbar v_F / \ell$.

We have four parameters that characterize the Coulomb energy W, J_{11}, J_{22} and J_{12}. At $d/\ell < \tilde{d}_c$ the largest of them is J_{11} (the intralayer exchange interaction in the graphene layer at the surface). Therefore, it is natural to consider the condition

$$J_{11} < \omega_c \tag{33}$$

as the additional restriction on the parameters. Eq. (33) can be rewritten as $\varepsilon > \varepsilon_c(d/\ell)$. The quantity ε_c can be understood as a critical dielectric constant. The dependence $\varepsilon_c(d/\ell)$ is also shown in Fig. 3.

Two conditions $d/\ell < \tilde{d}_c(\varepsilon)$ and $\varepsilon > \varepsilon_c(d/\ell)$ determine the range of parameters where one can expect a realization of electron-hole pairing and magnetoexciton superfluiduty in graphene bilayer systems.
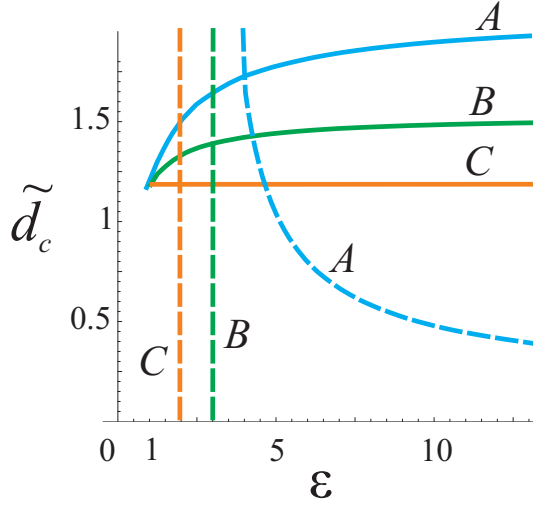
Fig. 3 Phase diagram at $\tilde{\nu}_a = 0$ for the graphene bilayers of A,B, and C type. Solid curves, $\tilde{d}_c(\varepsilon)$; dashed curves, $\varepsilon_c(d/\ell)$.

4 Critical temperature

In a bilayer graphene heterostructure with a fixed d the magnetoexciton superfluidity can be realized in a wide range of magnetic field. Variation of B at fixed gate voltage results in a change of imbalance of the active component. Simultaneous tuning of V_g allows to keep zero imbalance $\tilde{\nu}_a = 0$ and maximum order parameter under variation of B. In this section we study the dependence of critical temperature on magnetic field implying such a simultaneous tuning.

Superfluid transition temperature is given by the Berezinskii-Kosterlitz-Thouless equation [15]

$$T_c = \frac{\pi}{2}\rho_s(T_c), \tag{34}$$

where $\rho_s(T)$ is the superfluid stiffness at finite temperature. The superfluid stiffness is defined as the coefficient in the expansion of the free energy in the phase gradient $F = F_0 + \int d^2r \rho_s(\nabla\varphi)^2/2$. In a weakly nonideal Bose gas it is equal to $\rho_s = \hbar^2 n_s/m$, where n_s is the superfluid density. As was shown in previous section, superfluid stiffness determines also the supercurrent.

Taking into account linear excitations we present the free energy $F = E_0 - TS$ in the following form

$$F = E_0 + T\sum_{\mathbf{q}} \ln\left(1 - e^{-\frac{\Omega(\mathbf{q},\mathbf{Q})}{T}}\right). \tag{35}$$
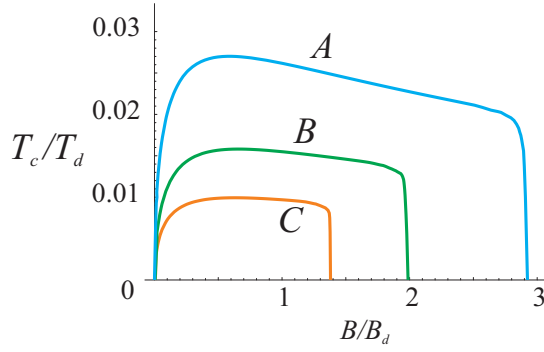
Fig. 4 Critical temperature vs magnetic field for A, B, and C structures. Temperature is given in units of $T_d = e^2/\varepsilon d$, magnetic field, in units of $B_d = \phi/\pi d^2$.

Expansion of Eq. (35) yields the following expression for the superfluid stiffness

$$\rho_s(T) = \rho_{s0} + \frac{1}{S}\sum_{\mathbf{q}}\left[\left(\frac{d^2\,\Omega(\mathbf{q},\mathbf{Q})}{dQ^2}\right)\Bigg|_{Q=0} N_q - \frac{1}{T}N_q(1+N_q)\left(\frac{d\Omega(\mathbf{q},\mathbf{Q})}{dQ}\right)^2\Bigg|_{Q=0}\right].$$
(36)

It follows from (36) and (29) that $\rho_s(T) < \rho_{s0}$ (thermal fluctuations reduce the superfluid stiffness).

For the spectrum $\Omega(\mathbf{q}) = E(q) + \hbar\mathbf{q}\mathbf{v}$ (where $\mathbf{v} = \hbar\nabla\varphi/m$ is the superfluid velocity) (36) yields the well-known answer for the superfluid density [28]. Eq. (36) generalizes the results [28] for the general case.

The dependence of critical temperature on magnetic field at $\tilde{\nu}_a = 0$ and $\varepsilon = 4$ is shown in Fig. 4. One can see that the maximum critical temperature is reached approximately at $B \approx 0.5B_d$, where $B_d = \phi/\pi d^2$ with $\phi = hc/2e$, the magnetic flux quantum.

5 Influence of impurities on the critical parameters

In the previous section we have determined the influence of thermal fluctuations on the superfluid stiffness. In this section we consider the effect of reduction of the superfluid stiffness caused by the interaction of magnetoexcitons with impurities.

The Hamiltonian of the interaction of the active component with impurities can be presented in the form

$$H_{imp} = \frac{1}{2S}\sum_{\mathbf{q}} U_z(\mathbf{q})\left(\hat{\rho}_1(\mathbf{q}) - \hat{\rho}_2(\mathbf{q})\right),$$
(37)

where $U_z(\mathbf{q}) = U_1(\mathbf{q}) - U_2(\mathbf{q})$, $U_i(\mathbf{q})$ is the Fourier-component of the impurity potential in the layer i, and

$$\hat{\rho}_i(\mathbf{q}) = \sum_X c^+_{i,X+\frac{q_y\ell^2}{2}}\, c_{i,X-\frac{q_y\ell^2}{2}} \exp\left(-iq_x X - \frac{q^2\ell^2}{4}\right)$$
(38)

is the Fourier component of the electron density operator for the active component.

In the state (13) the energy of interaction with the impurities expressed in terms of $m_z(q)$ reads as

$$E_{imp} = const + \sum_q \tilde{U}_z(q) m_z(q), \qquad (39)$$

where

$$\tilde{U}_z(q) = \frac{1}{\sqrt{2\pi \ell^2 S}} U_z(q \mathbf{i}_x) e^{-\frac{q^2 \ell^2}{4}}.$$

The interaction (39) induces the fluctuations of the density and the phase of the order parameter. Their values can be obtained from the Euler-Lagrange equations

$$\frac{\delta E}{\delta m_z(q)} = 0,$$
$$\frac{\delta E}{\delta \varphi(q)} = 0, \qquad (40)$$

where E is the energy of the system, described by the Hamiltonian $H = H_C + H_G + H_{imp}$ in the state (13).

Eqs. (40) solved in linear in impurity potential approximation yield

$$m_z(q) = -\frac{1}{2} \frac{K_{\varphi\varphi}(q) \tilde{U}_z(q\hat{\mathbf{x}})}{K_{zz}(q) K_{\varphi\varphi}(q) - K_{z\varphi}^2(q)}, \qquad (41)$$

$$\varphi(q) = \frac{i K_{z\varphi}(q) \tilde{U}_z(q\hat{\mathbf{x}})}{K_{zz}(q) K_{\varphi\varphi}(q) - K_{z\varphi}^2(q)}. \qquad (42)$$

Substituting (41), (42) into the expression for the energy one finds the correction to the energy caused by the electron-impurity interaction

$$\Delta E = -\frac{1}{4} \sum_q \tilde{U}_z(q) \tilde{U}_z(-q) \frac{K_{\varphi\varphi}(q)}{K_{zz}(q) K_{\varphi\varphi}(q) - K_{z\varphi}^2(q)}. \qquad (43)$$

In Eq. (43) the contribution of fluctuations with the wave vectors directed along x is taken into account. Summing the contribution for all wave vectors one obtains

$$\Delta E = -\frac{1}{8\pi \ell^2 S} \sum_{\mathbf{q}} U_z(\mathbf{q}) U_z(-\mathbf{q}) \frac{K_{\varphi\varphi}(\mathbf{q}, \mathbf{Q}) e^{-\frac{q^2 \ell^2}{2}}}{K_{zz}(\mathbf{q}, \mathbf{Q}) K_{\varphi\varphi}(\mathbf{q}, \mathbf{Q}) - K_{z\varphi}^2(\mathbf{q}, \mathbf{Q})}. \qquad (44)$$

For simplicity, we specify the case where impurities are located in graphene layers. Then the Fourier-component of the impurity potential can be presented in the form

$$U_z(\mathbf{q}) = \sum_a e^{i\mathbf{q}\mathbf{r}_a} u_{z,i}(\mathbf{q}), \qquad (45)$$

where $\mathbf{r}_a$ are the impurity coordinates, and $u_{z,i}(\mathbf{q}) = u_{1,i}(\mathbf{q}) - u_{2,i}(\mathbf{q})$ with $u_{k,i}(\mathbf{q})$, the potential in the layer k of a single impurity centered at $\mathbf{r} = 0$ in the layer i.

Averaging over impurities yields

$$\Delta E = -\frac{n_{imp}}{8\pi \ell^2} \sum_{\mathbf{q}} \left(|u_{z,1}(\mathbf{q})|^2 + |u_{z,2}(\mathbf{q})|^2 \right) \frac{K_{\varphi\varphi}(\mathbf{q}, \mathbf{Q}) e^{-\frac{q^2 \ell^2}{2}}}{K_{zz}(\mathbf{q}, \mathbf{Q}) K_{\varphi\varphi}(\mathbf{q}, \mathbf{Q}) - K_{z\varphi}^2(\mathbf{q}, \mathbf{Q})},$$
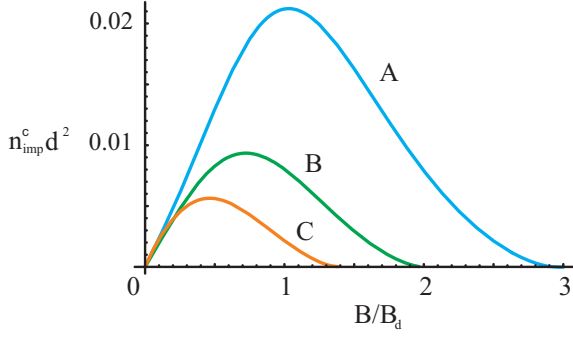$$(46)$$

Fig. 5 Critical impurity concentration vs magnetic field for charged impurities located in graphene layers.

where n_{imp} is the impurity concentration in a layer.

At $Q\ell \ll 1$ the energy (46) can be expanded in series as

$$\Delta E = \Delta E_0 + \frac{S}{2}\Delta\rho_s Q^2, \tag{47}$$

where

$$\Delta\rho_s = \frac{n_{imp}}{8\pi\ell^2 S}\sum_{\mathbf{q}} \frac{\left(|u_{z,1}(\mathbf{q})|^2 + |u_{z,2}(\mathbf{q})|^2\right)e^{-\frac{q^2\ell^2}{2}}}{K_{zz}^2(\mathbf{q},0)}\left(\left.\frac{\partial^2 K_{zz}(\mathbf{q},\mathbf{Q})}{\partial Q^2}\right|_{Q=0} - \frac{2\left(\left.\frac{\partial K_{z\varphi}(\mathbf{q},\mathbf{Q})}{\partial Q}\right|_{Q=0}\right)^2}{K_{\varphi\varphi}(\mathbf{q},0)}\right) \tag{48}$$

is the correction of the superfluid stiffness. One can check that the correction $\Delta\rho_s$ is negative. Thus, the interaction with impurities results in decrease of critical parameters.

At $\tilde{\nu}_a = 0$ Eq. (48) is reduced to

$$\Delta\rho_s = -\frac{n_{imp}}{S}\sum_{\mathbf{q}} \frac{\left(|u_{z,1}(\mathbf{q})|^2 + |u_{z,2}(\mathbf{q})|^2\right)e^{-\frac{q^2\ell^2}{2}}}{K_{zz}^2(\mathbf{q},0)}\left[\rho_{s0} - \frac{q^2 V_{12}(q)e^{-\frac{q^2\ell^2}{2}}}{32\pi^2}\right]. \tag{49}$$

where ρ_{s0} (Eq. (22)) is taken at $\theta_a = \pi/2$.

The shift of critical temperature is evaluated as $\Delta T_c/T_c \approx \Delta\rho_s/\rho_{s0}$[1]. We define the critical impurity concentration n_{imp}^c as a concentration at which $\Delta\rho_s/\rho_{s0} = 1$. We consider charged impurities with the potential $u_{z,ii}(\mathbf{q}) = (-1)^i(V_{12}(\mathbf{q}) - V_{ii}(\mathbf{q}))$. The dependence of critical impurity concentration on magnetic field at $\varepsilon = 4$ and $\tilde{\nu}_a = 0$ is shown in Fig. 5. We also evaluated critical concentrations for neutral impurities. These concentrations are much larger, and the influence of neutral impurities can be neglected.

---

[1] Since in our approach we assume smallness of $\Delta\rho_s/\rho_{s0}$ it is just an estimate

6 Conclusion

In conclusion, we present some estimates. Let us specify the type B structure (the one used in [1]) with $d = 20$ nm and $\varepsilon = 4$. For this structure the maximum critical temperature $T_c \approx 3$ K (in pure case) is reached in magnetic field $B \approx 0.8$ T. At such B the critical impurity concentration is $n_{imp}^c \approx 2 \cdot 10^9$ cm^{-2}. The gate voltage determined by Eq. (11) is $V_g \approx 6$ mV, that corresponds to electrostatic field $E \approx 3$ kV/cm.

Basing on the results of our study we may state the following.

1. Graphene bilayer structures are perspective objects for the observation of magnetoexciton superfluidity. The advantages are smaller magnetic fields and no restriction from above on physical interlayer distance, that means the possibility to suppress completely interlayer tunneling.

2. Gate voltage should be created between graphene layers for a realization of magnetoexciton superfluidity.

3. Certain conditions on dielectric constant and on the ratio between interlayer distance and magnetic length should be satisfied.

4. Structures with graphene layers situated at the surface have larger critical parameters.

5. Neutral impurities are not dangerous for the magnetoexciton superfluidity, but the concentration of charged impurities should be controlled.

References

1. Kim S, Jo I, Nah J, Yao Z, Banerjee SK, Tutuc E: **Coulomb drag of massless fermions in graphene**. *Phys. Rev. B* 2011, **83**: 161401(1-4).
2. Dean CR, Young AF, Meric I, Lee C, Wang L, Sorgenfrei S, Watanabe K, Taniguchi T, Kim P, Shepard KL, Hone J: **Boron nitride substrates for high-quality graphene electronics**. *Nature Nanotechnology* 2010 **5**: 722-726.
3. Lozovik YE, Sokolik AA: **Electron-hole pair condensation in a graphene bilayer**. *JETP Letters* 2008, **87**(1): 55-59.
4. Min H, Bistritzer R, Su JJ and MacDonald AH: **Room-temperature superfluidity in graphene bilayers**. *Phys. Rev. B* 2008, **78**: 121401(1-4).
5. Seradjeh B, Weber H, Franz M: **Vortices, Zero Modes, and Fractionalization in the Bilayer-Graphene Exciton Condensate**. *Phys. Rev. Lett.* 2008, **101**(24): 246404(1-4).
6. Berman OL, Lozovik YE, Gumbs G: **Bose-Einstein condensation and superfluidity of magnetoexcitons in bilayer graphene**. *Phys. Rev. B* 2008, **77**: 155433(1-10).
7. Lozovik YE, Merkulova SP, Sokolik AA: **Collective electron phenomena in graphene** *Phys. Usp.* 2008, **51**(7): 727-744.
8. Fil DV, Kravchenko LY: **Superconductivity of electron-hole pair in a bilayer graphene system in a quantizing magnetic field**. *Low Temp. Phys.* 2009, **35**: 712-723.
9. Bezuglyi, AI: **Dynamical equation for an electron-hole pair condensate in a system of two graphene layers**. *Low Temp. Phys.* 2010, **36**: 236-242.
10. Lozovik YE, Yudson VI: **Novel mechanism of superconductivity– pairing of spatially separated electrons and holes**. *Sov. Phys. JETP* 1976, **44**: 389-397.
11. Shevchenko SI: **Theory of superconductivity of systems with pairing of spatially separated electrons and holes**. *Sov. J. Low Temp. Phys.* 1976, **2**: 251-256.
12. Kellogg M, Eisenstein JP, Pfeiffer LN, West KW: **Vanishing Hall Resistance at High Magnetic Field in a Double-Layer Two-Dimensional Electron System**. *Phys. Rev. Lett.* 2004, **93**: 036801(1-4).

13. Wiersma RD, Lok JGS, Kraus S, W. Dietsche W, von Klitzing K, Schuh D, Bichler M, Tranitz HP, Wegscheider W: **Activated Transport in the Separate Layers that Form the $\nu_T = 1$ Exciton Condensate**. *Phys. Rev. Lett.* 2004, **93**: 266805(1-4).
14. Tutuc E, Shayegan M, Huse DA: **Counterflow Measurements in Strongly Correlated GaAs Hole Bilayers: Evidence for Electron-Hole Pairing**, *Phys. Rev. Lett.* 2004, **93**: 036802(1-4).
15. Moon K, Mori H, Yang K, Girvin SM, MacDonald AH, Zheng L, Yoshioka D, and Zhang SC **Spontaneous interlayer coherence in double-layer quantum Hall systems: Charged vortices and Kosterlitz-Thouless phase transitions**. *Phys. Rev.* B 1995, **51**: 5138-5170.
16. Eisenstein JP, MacDonald AH: **Bose-Einstein condensation of excitons in bilayer electron systems**. *Nature* 2004, **432**: 691-694.
17. Huse DA: **Resistance due to vortex motion in the $\nu = 1$ bilayer quantum Hall superfluid**. *Phys. Rev.* B 2005, **72**: 064514(1-4).
18. Roostaei B, Mullen KJ, Fertig HA, Simon SH: **Theory of Activated Transport in Bilayer Quantum Hall Systems**. *Phys. Rev. Lett.* 2008, **101**: 046804(1-4).
19. Fil DV, Shevchenko SI: **Transport properties of $\nu = 1$ quantum Hall bilayers. Phenomenological description**. *Phys. Lett.* A 2010, **374**: 3335-3340.
20. Yoon Y, Tiemann L, Schmult S, Dietsche W, von Klitzing K, Wegscheider W: **Interlayer Tunneling in Counterflow Experiments on the Excitonic Condensate in Quantum Hall Bilayers**. *Phys. Rev. Lett.* 2010, **104**: 116802(1-4).
21. Fil DV: **Locking and unlocking of the counterflow transport in $\nu = 1$ quantum Hall bilayers by tilting of magnetic field**. *Phys. Rev.* B 2010, **82**: 193303(1-4).
22. Fil DV, Shevchenko SI: **Interlayer tunneling and the problem of superfluidity in bilayer quantum Hall systems**. *Low Temp. Phys.* 2007, **33**: 780-782.
23. Su JJ, MacDonald AH: **How to make a bilayer exciton condensate flow**. *Nature Physics* 2008, **4**: 799-802.
24. Fil DV, Shevchenko SI: **Josephson vortex motion as a source for dissipation of superflow of e-h pairs in bilayers**. *J. Phys.: Condens. Matter* 2009, **21**: 215701(1-9).
25. Castro Neto AH, Guinea F, Peres NM, Novoselov KS, Geim AK: **The electronic properties of graphene**. *Rev. Mod. Phys.* 2009, **81**: 109-162.
26. Novoselov KS, McCann E, Morozov SV, Fal'ko VI, Katsnelson MI, Zeitler U, Jiang D, Schedin F, Geim AK: **Unconventional quantum Hall effect and Berrys phase of 2π in bilayer graphene.** *Nature Physics* 2006, **2**: 177 - 180.
27. Kravchenko LY, Fil DV: **Critical currents and giant non-dissipative drag for superfluid electronhole pairs in quantum Hall multilayers.** *J. Phys.: Condens. Matter* 2008, **20**: 325325(1-9).
28. Lifshitz EM, Pitaevskii LP: Statistical Physics, Part 2. Pergamon Press, 1980.